J. Fluid Mech. (1979), *vol.* 93, *part* 1, *pp.* 65–81
Printed in Great Britain

Overstability and inverted bifurcation in homeotropic nematics heated from below

By E. GUYON,
Laboratoire de Physique des Solides, Université Paris-Sud, 91405 Orsay
P. PIERANSKI AND J. SALAN
E.S.P.C.I. 10, rue Vauquelin, 75005 Paris

(Received 13 June 1978)

In nematic homeotropic films (director **n** perpendicular to the horizontal limiting plates) heated from below, the distortion of the director which is coupled to the ordinary heat convection mechanism responsible for the Rayleigh–Bénard instability exerts a strongly stabilizing influence. Owing to the difference in time scales, an oscillatory instability results whose characteristics are investigated experimentally here. An inverted bifurcation with an associated hysteresis is also obtained and this was studied in some detail. A vertical magnetic field H is also used to align the sample. The decrease of the orientational time constant when H increases leads to marked changes in the overstable regime, which are well described by a simple analysis.

1. Introduction

The nematic liquid-crystal state is an intermediate or meso-phase obtained below the isotropic liquid phase in some liquids composed of elongated molecules. In the nematic phase the centres of gravity of the molecules are distributed randomly but the molecules are locally aligned around an average direction characterized by a unit vector, the director $\mathbf{n}(\mathbf{r})$. Uniform molecular alignment in space ($\mathbf{n}(\mathbf{r}) = \mathbf{n}_0$) can be obtained by a surface treatment of the limiting surfaces of the cell containing the material. (However, not all geometries are suitable. In a cylindrical capillary tube with a molecular alignment perpendicular to the wall (homeotropic alignment) a line of defects develops along the axis of the cylinder which will affect the hydrodynamic behaviour.) One can also align the nematic along the direction of moderately large magnetic fields (**n** parallel to **H**).

Nematics flow easily (the viscosity is in the range of 10^{-1}–10^{-2} poise) and the extensive recent experimental studies fit well with the hydrodynamic theory established by Leslie and Ericksen and complemented by Parodi. The interested reader will find an extensive presentation of the physics of liquid crystal in the book of de Gennes (1974) and in several recent review articles on the hydrodynamics of nematics such as Jenkins (1978) and Dubois-Violette *et al.* (1978). Dubois-Violette & Manneville (1978) discuss theoretically the problem of cylindrical Couette flow instabilities in nematics and describe nematodynamics in an appendix. The notations are consistent with those used here.

The experiments presented here were done on MBBA (methoxybenzilidene-*p*-*n*-butylaniline), a classic material which has a nematic phase between 17 and 47 °C and

0022-1120/79/4232-6670 $02.00

which is commercially available. The experiments were carried out around a mean temperature of 25 °C. The material is contained between parallel horizontal plates coated with a surfactant (lecithin) to introduce a *homeotropic* alignment (**n** perpendicular to the plates). As the cell thickness in the experiment is rather large ($d \sim 5$ mm), a magnetic field perpendicular to the glass plates is also used to improve the homogeneity of alignment.

Thermal convection effects in such well-oriented horizontal nematic layers are drastically different from those obtained in homogeneous isotropic fluid layers heated from below (Normand, Pomeau & Velarde 1977). A most spectacular effect is the existence of a linear instability mode obtained in thick enough homeotropic films aligned by surface treatment and heated from *above* (Pieranski, Dubois-Violette & Guyon 1973). This instability has a fairly low threshold $\Delta T = T_U - T_L \sim (5/d^3)$, where d is the film thickness in mms, T_U and T_L refer to the temperature of the upper and lower plates. This case is rather unique in homogeneous materials as the density stratification is stable for such a sign of temperature gradient (the expansion coefficient $\alpha = V^{-1}\,\partial V/\partial T$) is positive). The existence of such an instability rests on the coupling between the flow induced by the buoyant force due to an initial temperature fluctuation and a distortion of **n** created by gradients of this flow field. The heat conductivity of nematics is anisotropic ($k_a = k_\parallel - k_\perp$ is positive; $\parallel$ and $\perp$ refer to the direction of the heat flux lines with respect to **n**) and the sense of the deflexion of the heat flux along the direction of **n** is such that the initial temperature fluctuation is reinforced. A physical reason for the existence of instability with a low threshold in this case as well as in purely hydrodynamic examples (Pieranski & Guyon 1974) can be found from a comparison of the time constants involved. The relaxation time of a velocity fluctuation, or more precisely a vorticity fluctuation, characterized by the dynamic viscosity ν, as well as that of a temperature fluctuation measured by heat diffusivity κ are rather fast. (In nematics, typical time constants for a thickness $d = 1$ mm are $t_v \sim d^2/\pi^2\nu = 10^{-2}$ s, $t_t \sim d^2/\pi^2\kappa \sim 1$ s.) On the other hand, the diffusive relaxation of a fluctuation of orientation taking place under the influence of the rather weak effect of an elastic torque (measured by a Frank elastic constant K) opposed by viscous torques (measured by a rotational viscosity γ) is rather slow, $t_0 = \gamma d^2/\pi^2 K \sim 10^3$ s for $d = 1$ mm. As usual in hydrodynamics, it is the existence of slowly diffusive processes which ensures the existence of low instability thresholds.

Quite recently, Lekkerkerker (1977) has pointed out that, in the homeotropic configuration used in the experiments of Pieranski, Dubois-Violette & Guyon (1973) if the nematic is heated from below, one does not expect the unfavourable coupling of the convective flow field with the director to increase the threshold above an isotropic value but rather to give rise to an oscillatory instability (overstability) above threshold. This possibility comes from the existence of a time scale from the relaxation of orientation t_0, which is associated with the stabilizing mechanism, large compared with the thermal time constant t_t which connects with the destabilizing buoyancy force, which controls the isotropic mechanism. There is a phase lag between the orientation and temperature fluctuations which permits the occurrence of the destabilizing buoyancy effect together with the stabilizing orientational heat defocusing effect.

Overstability has been discussed previously in the context of double diffusive phenomena (convection with a vertical gradient of composition as well as with a

temperature gradient). The relevant case is one in which a dense and more slowly diffusive component is at the bottom (stabilizing role) while the system is heated from below (destabilizing). In this problem, the existence of a molecular-diffusion time constant long compared with the thermal one gives rise to overstability above a critical temperature gradient. The stable density stratification can be created during the filling of the cell with the solution (Turner 1974) by using a mixture with the appropriate sign of Soret effect (which is the linear relation between the temperature gradient and the flux of matter). Two types of oscillations can then be obtained. Oscillations of steady amplitude (Platten & Chavepeyer (1972) were connected later (Hurle & Jakeman 1973) to effects possibly related to the cell geometry (oscillations were also obtained with pure liquids!). A possible mechanism involving the existence of a roll-cell circulation was related with a model by Busse (1972) describing an oscillatory instability connected with vertical vorticity, a simple picture of the oscillation being a wave travelling along the axis of the convection rolls. The instability is obtained with low-Prandtl-number fluids (however, in nematics the Prandtl number $P \sim 10^2$). Transient overstable oscillations were also obtained but only with the correct sign of Soret effect (see Hurle & Jakeman 1971; Platten & Chavepeyer, 1977). Above threshold, the amplitude of the oscillation grows until a finite-amplitude mode is triggered. In this problem, the overstable mechanism (obtained in a linear analysis) is also associated with an inverse bifurcation (which can be described from a nonlinear description such as the numerical model of Platten & Chavepeyer (1977). The present experiments agree with this last type of description. Oscillations are observed which agree with the linear analysis of Lekkerkerker (1977). In addition, characteristics of an inverted bifurcation similar to those of Platten & Chavepeyer (1977) are obtained. An original feature of the present study using nematics is the possibility of varying the orientational time constant by several orders of magnitude by applying a magnetic field. In particular, it is possible to reduce t_0 to values of the order of t_t. The variation of threshold and period of oscillations are well described by a simple one-dimensional analysis, presented in §3, which reproduces the results of Lekkerkerker's analysis and also includes the effect of a stabilizing field. The results of the experiments presented in §2 are analysed in the light of the theoretical analysis in §4.

2. Experiments

The convective flow cell containing the MBBA nematic liquid is shown in figure 1. The temperature gradient is created by circulating water at two different regulated temperatures on the outer faces of the nematic cell. We used two transparent 1 mm thick sapphire plates. The heat conductivity of the plates was of the order of 30 times larger than that of the 5 mm thick nematic film. This is an important precaution in order to ensure constant temperature boundary conditions: some relaxation oscillations in thermal convection have been connected with a weaker 'constant heat flux' boundary condition when poorly conducting limiting plates were used (see Platten, Chavepayer & Tellier 1973).

The homeotropic alignment of the nematic was obtained by precoating the inner faces of the plates with a thin lecithin film. We were not able to obtain a satisfactory uniform alignment on the thick films used (although 1 mm thick films could be well aligned using this technique) and the effect of a vertical magnetic field obtained from a

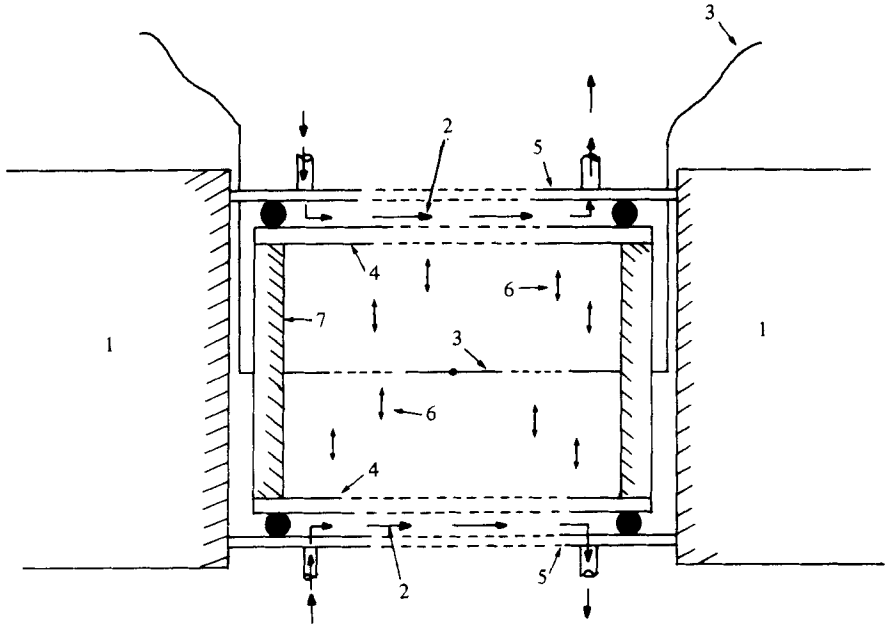

FIGURE 1. Experimental apparatus. The convective cell is contained in a coil (1) providing a vertical magnetic field. The water circulation (2) takes place between transparent glass (5) and sapphire (4) plates. The liquid crystal within the cell is homeotropic (6). Thermocouples (3) stretched across the cell and held to the 5 mm thick nylon spacer (7) are used to characterize the oscillating behaviour.

coil wound around the sample was added. With fields H larger than 30 G, a very homogeneous alignment is obtained. This is verified by the observation of the characteristic conoscopic image obtained in converging monochromatic light between crossed polarizers (Hartshorne & Stuart 1970).

Another test of the quality of the initial alignment was provided by studying the convection in the same 5 mm thick cell, heated from *above*. The critical threshold for this convection mode (discussed by Pieranski, Dubois-Violette & Guyon, 1973) increases quadratically with the applied stabilizing field, as expected (see figure 2). The extrapolated threshold for $H = 0$ is very small (less than 0·1 °C) as expected from the analysis of Dubois-Violette (1974) and the results obtained on a 1 mm thick cell (Pieranski, Dubois-Violette & Guyon 1973). However, the data obtained for fields smaller than 30 G are erratic, which indicates that the field is no longer able to oppose the spontaneous misalignment of the liquid crystal.

The thickness was defined by a 5 mm thick nylon spacer. A series of parallel 80 μm thick chromel–alumel thermocouples was stretched across the cell at its mid-plane. The existence of the wires did not modify appreciably the onset of convection from regions where no wires were present. However, above threshold, the geometry of the rolls tends to adjust in such a way as to minimize the gradients along the direction of the wires.

In the experiments the thermocouples were connected in pairs in a differential set-up. This was done in order to minimize the average temperature effects (in particular, the oscillations due to the water circulation regulation are of the order of 0·01 °C).

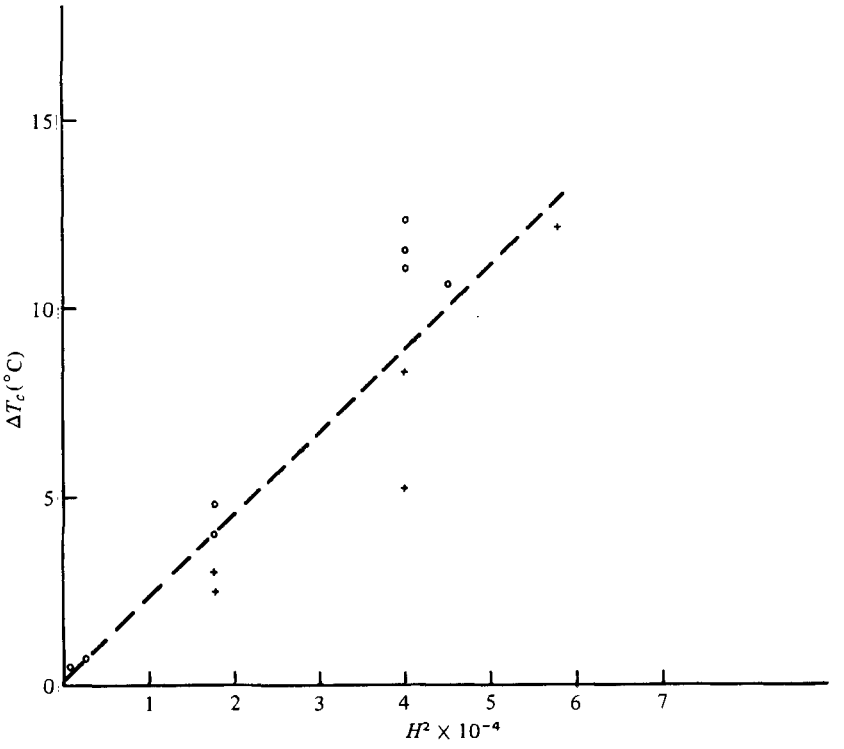

FIGURE 2. Variation of the threshold ΔT_c obtained while heating from above in the presence of a vertical (stabilizing) magnetic field. The crosses correspond to the absence of convection and the circles to the presence of it, as detected by visual inspection.

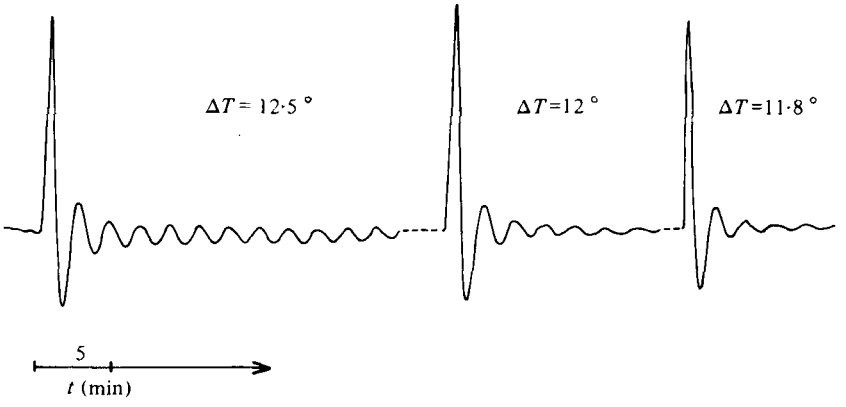

FIGURE 3. Response of a thermocouple to a short ($\sim$ 30 s) heat pulse applied to a nearby wire. The decay time constant of the oscillation decreases as the threshold ($\Delta T_c \sim 12{\cdot}6°$) is approached from below. The field H = 465 G.

The signal of the thermocouple was amplified using a Tekelec 925 nanovoltmeter and plotted on a set recorder. A typical curve is given in figure 3 in the presence of a vertical gradient just below the linear threshold. Initially, no instability is visible in the cell. A non-zero differential thermocouple indication comes from the fact that the thermocouples are not exactly in the same horizontal plane, which results in a small residual

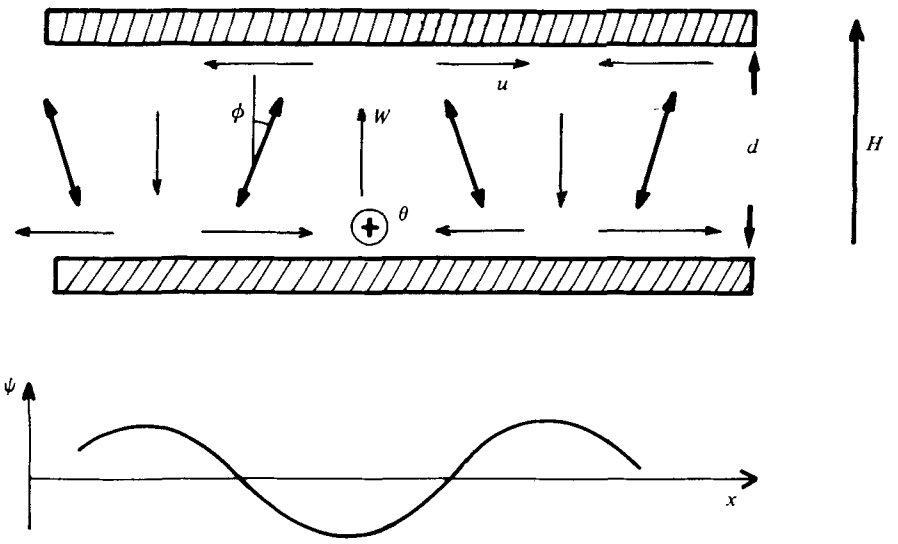

FIGURE 4. The director orientation and the curvature $\psi = d\phi/dx$ in the presence of a vertical velocity fluctuation w and temperature fluctuation θ. There is a de-phasing between ψ and w or θ not indicated in the figure.

vertical temperature difference. At time $t = 0$, a short (30 s) heat pulse is applied on a resistive wire parallel to the two differential thermocouples. A pair of rolls is induced in symmetrical positions parallel to the wire. When the heat is suppressed, the oscillation detected across the thermocouple is characteristic of the overstable behaviour as discussed below. Convection is easily detected optically. However, optical tests are not easily performed because of the high interference orders obtained even for small distortions (a distortion of 1 degree from homeotropic alignment corresponds to an optical path difference of 0·2 μm) and we will use only thermal thresholds although the order of magnitude and the nature of the effects obtained with both types of measurement agree.

3. Model

Rather than reproduce the analysis of Lekkerkerker (1977), we present a simple, although incomplete, approach based on a one-dimensional model which emphasizes the physical features of the problem in terms of the time constants. It also provides a first analysis of the behaviour in the presence of a magnetic field. Equations are similar to those introduced by Dubois-Violette, Guyon & Pieranski (1975). We consider the coupled interplay of fluctuations in the temperature θ, the vertical component of the velocity w and the curvature $\psi = d\phi/dx$ (the variables are defined in figure 4), retaining only their sinusoidal dependence in x, i.e.

$$\theta/\theta_0 = w/w_0 = \psi/\psi_0 = \exp(iqx),$$

with a single mode $q = \pi/d$ (experiments show that the size of the rolls is nearly equal to the thickness of the cell). We use the reduced variables

$$\tilde{w} = w_0/\kappa_\perp q, \quad \tilde{t} = t\kappa_\perp q^2, \quad \tilde{\psi} = \psi_0/q, \quad \tilde{\theta} = -\theta_0 q/\beta.$$

We note that $\beta = \partial T/\partial z$ is negative when heat is supplied from below.

The following set of equations is obtained:

$$\partial\tilde{w}/\partial\tilde{t} = -P\tilde{w} + R'P\tilde{\theta}, \tag{1}$$

$$\partial\tilde{\theta}/\partial\tilde{t} = -\tilde{\theta} + \tilde{w} - X\tilde{\psi}, \tag{2}$$

$$\partial\tilde{\psi}/\partial\tilde{t} = -\zeta\tilde{\psi} + \tilde{w}. \tag{3}$$

The Prandtl number $P = \nu/\kappa \sim 10^2$. The velocity will follow the temperature fluctuation with the time scale $(\kappa_\perp q^2)^{-1}$. The Rayleigh number is $R' = -g\alpha\beta/\kappa_\perp \nu q^4$. (This definition is $\sim 10^{-2}$ of the usual definition $R = -g\alpha\beta d^4/\kappa_\perp \nu$). The parameters

$$X = \kappa_a/\kappa_\perp, \quad \zeta = (Kq^2 + \chi_a H^2)/(\gamma\kappa_\perp q^2) \tag{4), (5}$$

are characteristics of the nematic state. X is the ratio of the anisotropic part of the heat diffusivity ($\kappa_a = \kappa_\parallel - \kappa_\perp$) to that perpendicular to the molecules $\kappa_\perp$. It is of the order 0·7 in MBBA (Villanove *et al.* 1974); ζ is the ratio of the thermal time constant t_t to the orientational one $t_0(H) = \gamma/(Kq^2 + \chi_a H^2)$. (The formula for $t_0(H)$ generalizes the expression of t_0, given above, in the case where a magnetic field H is applied along $\mathbf{n}$. The effect of H is to stabilize $\mathbf{n}$ and thus reduce the relaxation time constant towards equilibrium.) The ratio ζ is small compared with 1 in the absence of a field (typically $\sim 10^{-3}$). However, it becomes of order 1 for moderate values of the vertical (stabilizing) field: $\zeta = 1$ for $H \sim 500$ G and $d = 5$ mm.

In the isotropic state the equations reduce to the Navier–Stokes equation (1) and to the heat equation (2) without the $X\tilde{\psi}$ term. The coupling is through the buoyancy effect $R'P\tilde{\theta}$ and the convective term $\tilde{w}$. Assuming the principle of exchange of stabilities, $\tilde{w}, \tilde{\theta} \propto \exp(st)$ with $s = 0^+$ for $R' = R'_c$, we get the compatibility condition

$$(-P + R'_c P)\,\tilde{\theta} = 0 \quad \text{or} \quad R'_c = 1, \tag{6}$$

which is of the order of magnitude of the exact threshold with free boundaries ($R'_c \sim 6{\cdot}7$ to 10 depending on the thermal boundary conditions).

The equations in the nematic state are a one-dimensional transposition of the two-dimensional equations which come directly from linear hydrodynamic theory. Rather than reproduce a formal derivation we shall give a phenomenological description of the equation (Dubois-Violette 1974). The term $-\chi\tilde{\psi}$ accounts for the focusing mechanism due to the anisotropy of heat conductivity. One can see easily on figure 4 that in the central region $\psi < 0$ the heat flux is deflected towards the centre ($+\theta$ point) if heat is supplied from below and if the heat diffusivity anisotropy, κ_a is positive. The new equation (3) describes the relaxation of the director. In the absence of coupling (neglecting $\tilde{w}$ term) the equation expresses the diffusive relaxation of the director with a time constant t_0 as it can be checked easily by using natural units. The additional term $\tilde{w}$ expresses the coupling between the flow pattern and the distortion: in fact the dominant contribution to the hydrodynamic torque is $\alpha_2\,\partial u/\partial z$ which comes from the gradient of u, the horizontal component of the velocity, and is larger than the contribution $\alpha_3\,\partial w/\partial x$ due to the gradient of w, the vertical component. α_2 and α_3 ($|\alpha_3| \ll |\alpha_2|$) have the dimension of viscosity (de Gennes 1974). In the case in the figure the hydrodynamic torque $\alpha_2\,\partial u/\partial z$ exerts a stabilizing role, i.e. tends to reduce the distortion. Qualitatively one could say that the heat-focusing action and flow-coupling effect tend

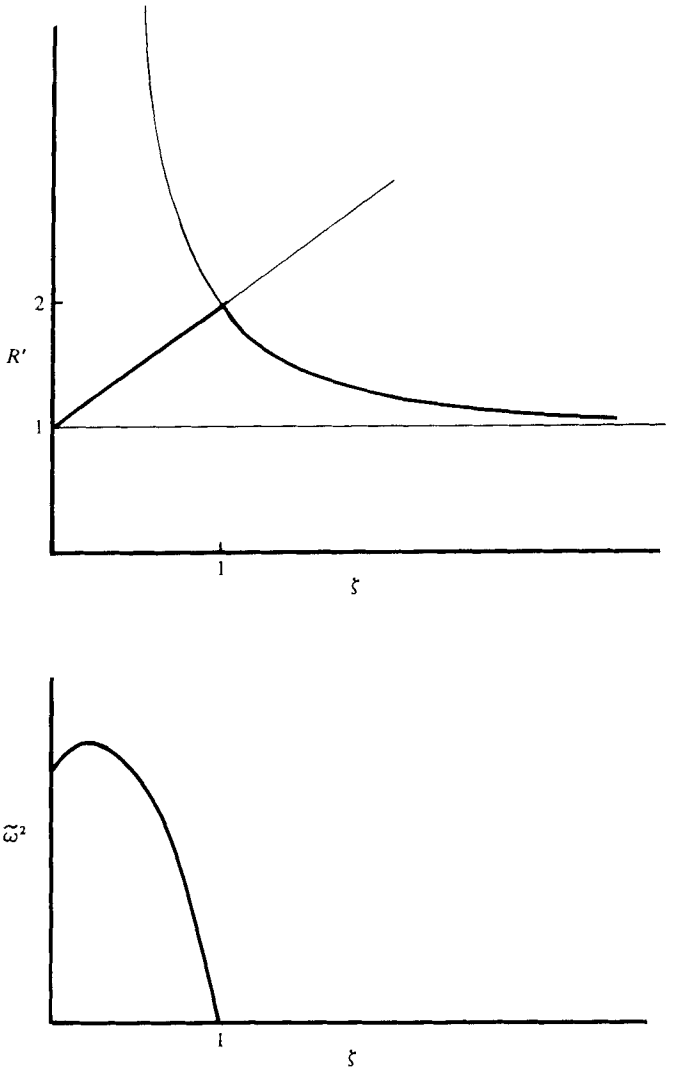

FIGURE 5. Variation of the reduced Rayleigh number R' and frequency of oscillation $\tilde{\omega}$ as a function of the quantity ζ defined in (5).

to oppose each other. One could see in very similar terms that if heat had been supplied from above (which would amount to replacing $an+\theta$ effect by $an-\theta$ effect from heat focusing) this mechanism and the flow coupling would have acted in the same sense, permitting the convection which is observed in homeotropic films heated from above. Using the result of the above discussion, one obtains the last term of equation (3) by replacing first $\partial u/\partial z$ by $-\partial w/\partial x$ (a valid approximation for circular rolls) and by using the fact that the ratio $-\alpha_2/\gamma$, which comes from the balance between the hydrodynamic torque $\alpha_2 \partial w/\partial x$ and the viscous one $\gamma \partial\psi/\partial t$, is very nearly equal to one.

We now assume in (1)–(3) a hierarchy of time constants such that $P \gg 1$ or ζ. Under these conditions, the velocity fluctuations follow the thermal ones and a solution of the set of equations can be obtained by setting $\partial/\partial t = 0$ in (1) (an opposite limit $\zeta \gg 1$ or P,

obtained in very large fields, could be solved similarly by setting $\partial/\partial t = 0$ in (3) with drastically different results). We get:

$$\partial^2\tilde{\psi}/\partial\tilde{t}^2 + [\zeta + 1 - R']\,\partial\tilde{\psi}/\partial\tilde{t} + [\zeta(1-R') + XR']\,\tilde{\psi} = 0. \tag{7}$$

We look for solutions $\tilde{\psi} = \exp[s(R')\,t]$.

(i) If $\Delta = (\zeta - 1 + R')^2 - 4XR'$ is positive, the growth state $s(R')$ is real and vanishes at a threshold

$$R'_c = 1 + X/(\zeta - X), \tag{8}$$

which tends towards the isotropic value $R'_c = 1$ for large fields. In this regime, the diffusivity of orientation is fast compared with the thermal diffusivity and the director follows the velocity field. However, the distortion of the director is limited by the field, and the increase of threshold due to the destabilizing heat defocusing effect becomes negligible in large fields. The condition $\Delta > 0$ at threshold is first met for

$$\zeta_0 = \tfrac{1}{2}X + \tfrac{1}{2}(X^2 + 4X)^{\frac{1}{2}}. \tag{9}$$

For an anisotropy ratio $X = \frac{1}{2}$, we get $\zeta_0 = 1$. Inserting these values in (8) we get the smallest Rayleigh number giving a non-oscillating solution to be $R'_c = 2$. The variation of threshold above this value is a branch of the hyperbola on figure 5 which is a plot of R'_c *vs.* ζ (or, in physical terms, versus H^2):

(ii) If $\Delta < 0$, the quantity

$$s = \tfrac{1}{2}\{(R' - 1 - \zeta) \pm i(4XR' - (\zeta - 1 + R')^2)^{\frac{1}{2}}\}$$

is complex. The threshold is defined by

$$R'_c = 1 + \zeta, \tag{10}$$

and by putting this value in the imaginary part of s we get the frequency of the oscillation predicted by the linear theory at threshold:

$$\tilde{\omega} = 2\{-\zeta^2 + X(1+\zeta)\}^{\frac{1}{2}}. \tag{11}$$

One checks indeed that the frequency vanishes for $\zeta = \zeta_0$.

When the relaxation of the director is slow compared with the thermal relaxation ($\zeta \ll 1$) the oscillations of ψ are in quadrature with that of w and the distortion does not modify the threshold from the isotropic value. The mechanism is clearly emphasized in Lekkerkerker's paper (1977, figure 1) and resembles that obtained in the case of double diffusive phenomena where the density gradient is stabilizing against the unstable thermal one but has a much longer time scale. A new feature in the present problem is the possibility of adjustment of the ratio ζ. When ζ approaches ζ_0, the two time constants become of the same order and the oscillating mechanism becomes less efficient: the threshold increases. The variation of threshold and frequency with field is plotted on figure 5.

The results in zero field [taking $\zeta \sim 0$ in (11)] agree with the analysis of Lekkerkerker which gives the same threshold value and a frequency

$$\omega_c \sim q^2(\tfrac{1}{2}\kappa_a\kappa_\parallel)^{\frac{1}{2}},$$

which is within a factor of 2 of formula (11) if one uses the real time scale t.

Let us emphasize that the above linear analysis does not provide us with any

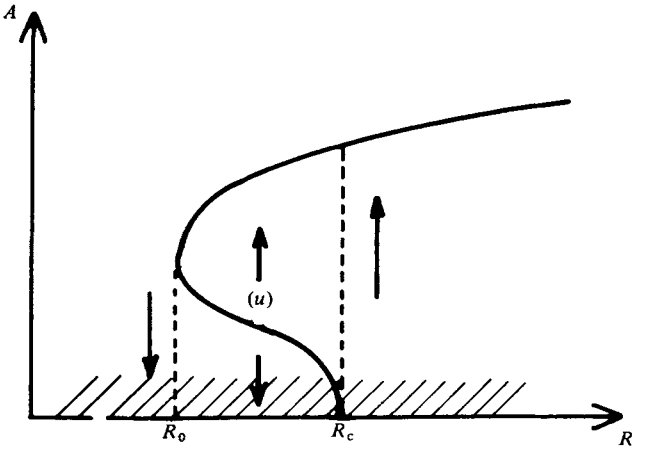

FIGURE 6. The variation of the amplitude of the temperature fluctuation as a function of the Rayleigh number R shown schematically. The arrows indicate the direction of spontaneous evolution of the system. The hatched region refers to the linear regime.

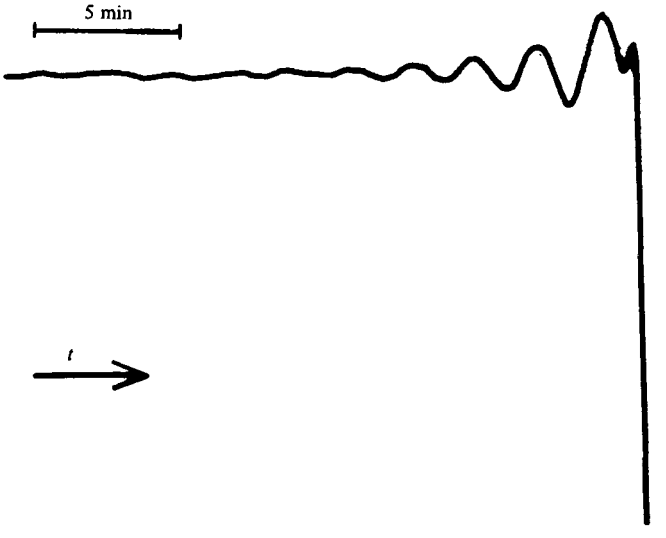

FIGURE 7. Spontaneous oscillating amplification of the instability for temperature gradients such that $R \gtrsim R_c$. The vertical line to the right corresponds to the irreversible evolution toward a strongly distorted state.

information about nonlinear effects. In particular, a nonlinear analysis similar to that performed by Platten & Chavepeyer (1977) would be needed in order to describe the finite-amplitude branches associated with an inverse bifurcation. As no such treatment exists in the nematic case, we use the results of the analysis of Platten & Chavepeyer (1977) for the Soret problem which are sketched in figure 6. The linear regime, corresponding to the treatment given above, applies only if the amplitude of the fluctuations is small enough. Moreover, it cannot give the sign of curvature of the linear branch next to R_c. Our results are consistent with an inverse bifurcation mechanism such that an hysteretic behaviour is found between R_0 and R_c when the gradient is increased or

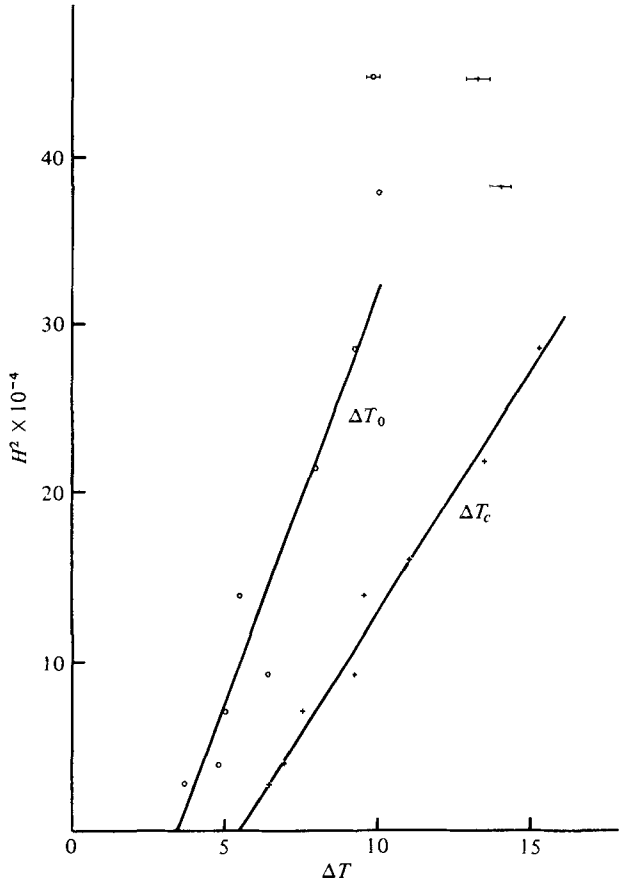

FIGURE 8. Variation of the critical thresholds. +, ΔT_c obtained in increasing gardient; ○, ΔT_0 obtained in decreasing gradient; both as a function of the applied field. The temperature is applied from below.

decreased. We can understand the switching over between the linear and nonlinear branch, qualitatively, as follows: as the amplitude of the oscillations increases, it eventually perturbs so strongly the director orientation that the distortion orientation no longer relaxes to zero and its unfavourable focusing contribution is lost. At the same time, the oscillation disappears. This is indeed confirmed by experiments.

4. Results and discussion

4.1. *Thresholds*

The temperature difference across the cell is very slowly *increased*. The value of the threshold is detected thermally by the occurrence of a transient oscillation followed by an irreversible change (decrease) of the temperature reading. An example of such variation is shown in figure 7. The decrease of temperature comes from the fact that, owing to convection, the temperature gradient in the bulk of the film decreases and the variation tends to be localized in boundary layers next to the wall. In the steady state obtained just above this transition the convective structure is seen with a strong optical

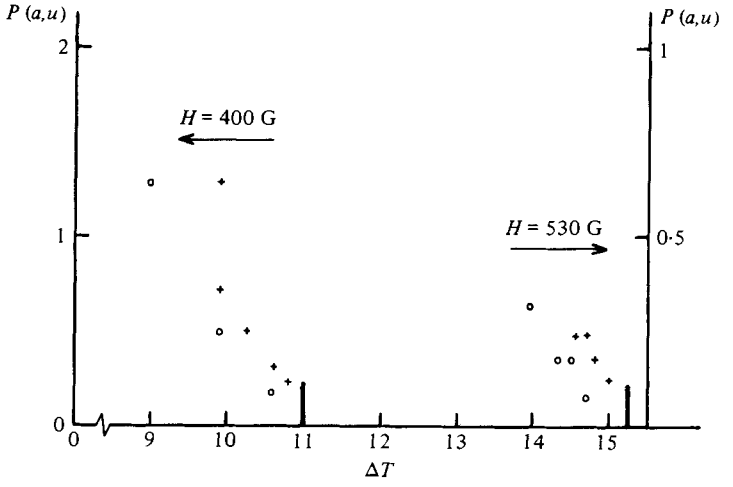

FIGURE 9. A heat pulse of constant duration and power P is applied to a wire in the cell. Circles indicate values too small to trigger the instability and crosses indicate values for which convection was initiated through the cell after the heat pulse. The heavy vertical line indicates the threshold value ΔT_c corresponding to the variation of figure 8. The variation should be analysed qualitatively as coming from the unstable branch (u) on the variation of figure 6.

contrast indicating that the distortion of the director is already quite large. We call ΔT_c the critical threshold thus obtained in increasing gradient.

Starting from such well-developed convection, the temperature difference is *decreased*. The convective image disappears only below a reduced value of the threshold ΔT_0. The decrease is also associated with a discontinuous change in the thermocouple reading. The values of ΔT_c and ΔT_0 obtained for different applied magnetic fields are given in figure 8.

There is no model to describe the linear variation of ΔT_0 which corresponds to the threshold R_0 of figure 5, but a dependence on H^2 is likely from the form of ζ in (5). For the largest value of field, $H = 650$ G, the thresholds decrease again. The maximum corresponds to a value $H_0 \sim 580$ G. The variation can be compared with that of figure 5 and we tend to associate the value H_0 with ζ_0 defined in (9).

This is also confirmed by the value of the ratio $\Delta T_c(H_0)/\Delta T_c(0)$ which we find experimentally to be of the order of 3. The numerical estimate using our simplified model gives a ratio of 2 for $\kappa_a/\kappa_\perp = 0{\cdot}5$ and 3 for $\kappa_a/\kappa_\perp = 1$; experimentally $\kappa_a/\kappa_\perp \sim 0{\cdot}7$ (Villanove *et al.* 1974). However, one cannot take the quantitative agreement too seriously, because the simplifications used in the one-dimensional analysis that extends the work of Lekkerkerker (1977) to account for the magnetic field dependence do not really permit a quantitative comparison.

4.2. *Hysteresis between ΔT_0 and ΔT_c (R_0 and R_c)*

If we increase the gradient to a value between ΔT_0 and ΔT_c, the ambient fluctuations do not reach sufficient amplitude to trigger the instability. One can initiate it by heating one of the wires stretched along the cell. If the heating power is small enough, we obtain a reversible change to the state of rest when the heat is suppressed. This is the result shown in figure 3. If the power supplied P is larger than a value depending on the

distance of ΔT to ΔT_c, we observe that the initial pair of rolls formed along the wire progressively invades the cell by inducing other parallel rolls. The structure does not relax to the undisturbed state if the heat is suppressed. There is an irreversible evolution to the finite-amplitude branch. Coming back to figure 6 we see that the linear unstable branch is a marginal line for the two types of evolution characterized by the down and up going arrows. Figure 9 gives the limit of instability for different applied powers P and shows a variation qualitatively similar to the unstable branch (u) of figure 6. Unfortunately, it is not possible, from the experiment, to connect in a simple way the applied power P to the amplitude A of the velocity fluctuation next to the wire; moreover the local temperature pattern is also modified by this heating. An experiment involving the inducing effect of fluctuations of orientation caused by local electric fields, which does not have such drawbacks, is under way.

4.3. *Oscillatory behaviour*

One can easily study the oscillations associated with the onset of instability by first setting the gradient to a fixed value ΔT in the presence of a large enough stabilizing field H_1 (such that $\Delta T < \Delta T_c(H_1)$) and decreasing H suddenly to a value H_2 just above threshold ($\Delta T > \Delta T_c(H_2)$). The oscillation can be detected most easily from the thermocouple reading, but it can also be seen optically by the periodic disappearance of the convective structure in the cell at least as long as the amplitude of the distortion remains small enough. Next to threshold, several oscillations are observed before the nonlinear branch is attained, whereas, farther from it, only one or two oscillations are detected. A systematic study of the increase of the growth rate for increasing gradients is cumbersome because the defects induced in the cell after a finite-amplitude instability has been reached do not relax rapidly to zero when the structure is erased by a large field.

We have considered in detail the variation of the time rate below threshold by the technique sketched in figure 2. The decay signal read on the thermocouple follows very nearly a law of the form

$$A \exp(-st) \cos \omega t, \tag{12}$$

where s and ω do not depend on the characteristics of the heat pulse as long as the power is small enough.

4.3.1. *Rate.* Figure 10 gives the variation of s with ΔT for $\Delta T < \Delta T_c$. It is consistent with a linear behaviour

$$s \propto |\Delta T_c - \Delta T|$$

characteristic of a mean-field-like behaviour (we deal with a decay process and s is negative). This is a rather inaccurate fit. Very near threshold, the simple law (12) is not obeyed and one observes the variation of figure 3 ($\Delta T = 12{\cdot}5\,^{\circ}\mathrm{C}$), where the amplitude first decreases and then remains constant for a long period of time; at the end, a finite-amplitude mode will be triggered, possibly because of some external fluctuations such as those coming from the temperature regulation. Farther from threshold (figure 3 ($\Delta T = 11{\cdot}8\,^{\circ}\mathrm{C}$)) the decay rate is too fast (typically when $s > \omega$) to lead to a meaningful estimate of s.

However, we wish to emphasize, at this point, that we have recovered, at least

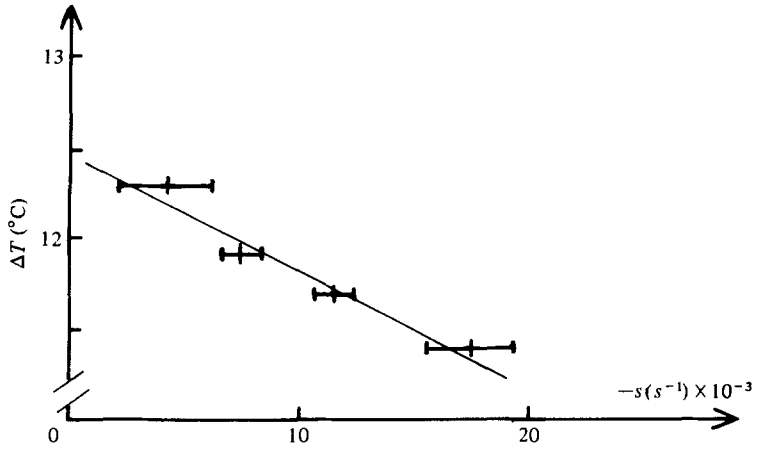

FIGURE 10. Variation of the decay rate with the applied temperature gradient below threshold for an applied field $H = 465$ G. Errors are larger both near ΔT_c ($s \to 0$) where an exponential decay is not well obeyed and far below ΔT_c where the decay is fast ($-s$ large).

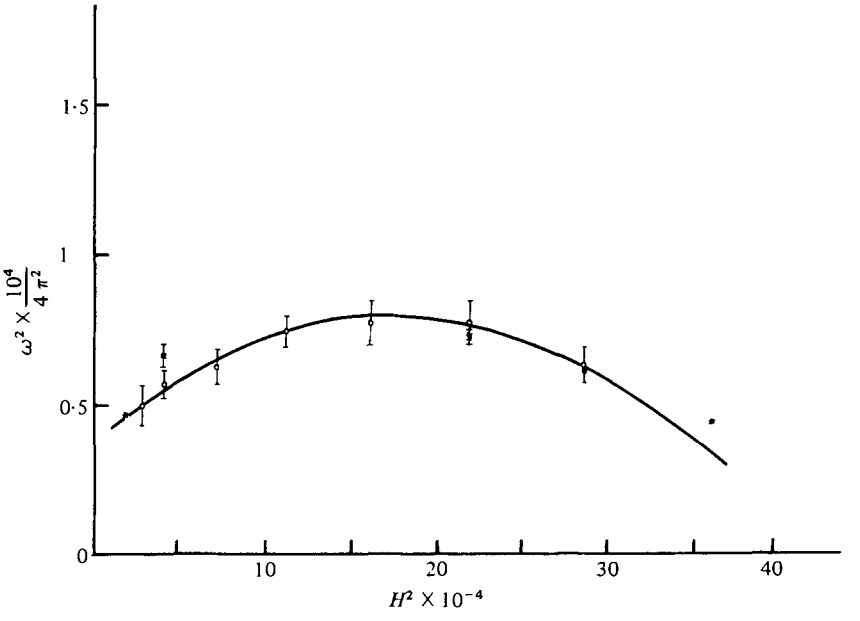

FIGURE 11. Variation of frequency ω of the oscillations versus applied field (compare with the lower curve of figure 5).

qualitatively, the essential characteristics expected from a linear analysis of the instability 'à la Landau' as was done beautifully in the case of direct bifurcation Rayleigh–Bénard instability by Weisfreid *et al.* (1978), despite the fact that the present problem is concerned with an inverse bifurcation. We may also note that, from the local heating experiment, we also get an indication of the increase of the two-dimensional correlation length as the threshold is approached from below. Instead of the single pair of rolls formed along a heated wire, a progressively larger spatial extent of instability is observed when ΔT is approached (typically three pairs of rolls are seen

when $\Delta T_c - \Delta T \sim 0{\cdot}3\,^{\circ}\mathrm{C}$). This feature will be analysed in detail in a further optical study.

4.3.2. *Period.* An accurate determination of the period can be obtained near ΔT_c because a large number of periods can be recorded. In the range of ΔT where several periods are visible, no appreciable variation of ω is detected. This is consistent with the overstable picture which states that the threshold of instability is obtained when the equations of motion for the Fourier amplitudes (1)–(3) (also Lekkerkerker 1977, equations 4, 5) develop a pair of complex conjugate roots $0 \pm i\omega$. Next to threshold, the eigenvalues of the problem $(s \pm i\omega)$ are such that s vanishes linearly at threshold whereas ω is finite and only varies linearly with the distance to threshold.

In figure 11 we have indicated the values of frequency ω for different values of fields H. The quasi-parabolic shape is strongly similar to the variation of figure 5. In particular, for the largest attainable threshold $\Delta T_c \sim 15^{\circ}$ and $H = 650$ G the oscillatory behaviour has disappeared. The behaviour fits well with the simple analysis given in §2. We can associate the field $H_0 = 580$ G which corresponds to the maximum of the critical gradient and is the first value such that $\omega = 0$ to the critical condition

$$t_0(H_0) = t_t.$$

The value of the field agrees reasonably well with the numerical estimate $H = 500$ G for $d = 5$ mm given in §3 using average values of MBBA. Thus both threshold and frequency variations fit with the picture of figure 5 at least up to H_0.

5. Conclusion

In this article we have outlined some essential characteristics of an overstable instability using experiments on nematics. Once more, nematic liquid crystals provide an original tool for the study of hydrodynamic instabilities. The anisotropic viscoelastic behaviour of liquid crystals is well known now and merely introduces some analytical difficulties which were not considered in this 'first generation' experiment. A main advantage in using, as a new variable, the director field is the fact that it can be acted upon easily by external fields. This feature has permitted a new approach to the overstability problem which enables us to control continuously within the same experiment the ratio of the two time constants involved. In particular, the quenching of the oscillations obtained when the ratio is of the order of 1 seems to be inaccessible to double-diffusive phenomena as the ratio κ/D (the Lewis number) is generally much larger than 1 in liquids. This variation provides a new way of distinguishing the overstability mechanism from the other causes of oscillations, met in Rayleigh–Bénard problems, that we had discussed in the introduction.

Another point of emphasis in this work has been the characterization of the properties of the instability around the linear threshold ΔT_c which does not seem to have been much studied in the Soret-effect experiments. This study is being pursued in Madrid by one of us (J. S.) along several lines indicated in the present work: the use of thicker cells (smaller gradients) will permit the description of the variations in the non-oscillating–quenched-oscillations range ($t_0(H) < t_T$). Emphasis will be put on the use of the director field itself both for the production of fluctuations to trigger the instability and for the characterization of the oscillations. This can be achieved by

interdigital electrodes deposited on the limiting plates, using capacitive techniques in a manner comparable with the Prost experiments (Prost & Pershan 1976).

The present work is dedicated to the memory of Jean-Claude Lacroix whose beautiful Ph.D. work (1976) on the inverse bifurcation in electrohydrodynamic convection in liquids submitted to unipolar injection has provided us with a remarkable example of inverse bifurcation in convective phenomena.

We thank Drs Velarde and Lekkerkerker for several illuminating discussions on this problem.

Note. It has been pointed out to us by one of the referees that in the set of equations (1)–(3) describing the coupling between velocity, temperature and orientation, one term, present in the analysis of Lekkerkerker (1977) and describing a linear coupling between the curvature of the distortion $\tilde{\psi}$ and the acceleration $\partial\tilde{w}/\partial\tilde{t}$, is missing. Our analysis in fact reproduces that given by Dubois–Violette (1974), for example, which considers the threshold for stationary instabilities ($\partial\psi/\partial t = 0$). In the present problem, dealing with a non-stationary instability, the rotation of $\mathbf{n}(\partial\psi/\partial t \neq 0)$ induces a flow field. (This 'back-flow effect' was observed and discussed in particular in the article by Pieranski, Brochard & Guyon (1973). This effect gives in (1) a contribution proportional to $\alpha_3\,\tilde{\psi}$, where α_3 is a viscosity term. Eliminating this term using (3), we see that the consideration of 'back flow' has two effects: (i) It renormalizes the viscosity (modifies the factor $P\tilde{w}$ in (1)). As some flow is taking place as well as the director rotation, a reduced viscosity is usually obtained. Such an effect was analysed in detail in the above reference. (ii) It introduces in (1) a contribution proportional to $\tilde{\psi}$. However, as the time constant of the oscillation (measured by t_t) is much smaller than the natural time constant of the director (t_0), it can be seen easily that the second contribution is small.

After the submission of this article, an analytical description of the effect of the field of threshold was proposed by Lekkerkerker (to be published). His results agree well with our analysis leading to figure 5. He finds that in a large magnetic field (ζ large) the value of threshold R' is 10 % larger than the value for $\zeta = 0$. The difference is due to the consideration of the backflow term. In a recent numerical analysis by Zunega & Velarde (to be published) based on a Galerkin solution of various thermal convective problems in nematics, the same results as figure 5 were analysed following our first approach.

REFERENCES

Busse, F. H. 1972 Oscillatory instability of convection rolls in a low Prandtl fluid. *J. Fluid Mech.* **52**, 97.

Dubois-Violette, E. 1974 Determination of thermal instabilities threshold for homeotropic and planar nematic liquid crystal samples. *Solid State Comm.* **14**, 767.

Dubois-Violette, E., Durand, G., Guyon, E., Manneville, P. & Pieranski, P. To appear in a supplement to *Solid State Physics* (special issue on liquid crystals).

Dubois-Violette, E., Guyon, E. & Pieranski, P. 1975 Heat convection in a nematic liquid crystal. *Mol. Cryst. Liq. Cryst.* **26**, 193.

Dubois-Violette, E. & Manneville, P. 1978 Stability of Couette flow in nematic liquid crystals. *J. Fluid Mech.* **89**, 273.

Gennes, P. G. de 1974 *The Physics of Liquid Crystals*, chap. 5. Oxford: Clarendon Press.

Hartshorne, N. H. & Stuart, A. 1970 *Crystals and the Polarizing Microscope.* London: Edward Arnold.

HURLE, D. T. J. & JAKEMAN, E. 1971 Soret-driven thermosolutal convection. *J. Fluid Mech.* **47**, 667.

HURLE, D. T. J. & JAKEMAN, E. 1973 Thermal oscillations in convecting fluids. *Phys. Fluids* **16**, 2056.

JENKINS, J. T. 1978 Flows of nematic liquid crystals. *Ann Rev. Fluid Mech.* **10**, 197.

LACROIX, J. C. 1976 Instabilités hydrodynamiques et électroconvection lors d'injection d'ions dans les liquides isolants. Thèse de Doctorat, Grenoble.

LEKKERKERKER, H. N. W. 1977 Oscillatory convective instabilities in nematic liquid crystals. *J. Phys. Lett.* **38**, L 277.

LESLIE, F. M. To be published in *Advances in Liquid Crystals.*

NORMAND, C., POMEAU, Y. & VELARDE, M. G. 1977 Convective instability: a physicist's approach. *Rev. Mod. Phys.* **49**, 581.

PIERANSKI, P., BROCHARD, F. & GUYON, E. 1973 Static and dynamic behaviour of a nematic liquid crystal in a magnetic field. Part II: dynamics. *J. Phys.* **34**, 35.

PIERANSKI, P., DUBOIS-VIOLETTE, E. & GUYON, E. 1973 Heat convection in liquid crystals heated from above. *Phys. Rev. Lett.* **30**, 736.

PIERANSKI, P. & GUYON, E. 1974 Instability of certain shear flows in nematic liquids. *Phys. Rev.* A **9**, 404.

PLATTEN, J. K. & CHAVEPEYER, G. 1972 Oscillations in a water–ethanol liquid layer heated from below. *Phys. Lett.* A **40**, 287.

PLATTEN, J. K. & CHAVEPEYER, G. 1977 Nonlinear two dimensional Bénard convection with Soret effect: free boundaries. *Int. J. Heat. Mass Transfer.* **20**, 113.

PLATTEF, J. K., CHAVEPEYER, G. & TELLIER, J. 1973 Finite amplitude oscillatory motion in the two component Bénard problem. *Phys. Lett.* A **44**, 479.

PROST, J. & PERSHAN, P. S. 1976 Flexoelectricity in nematic and smectic A liquid crystals. *J. Appl. Phys.* **47**, 2298.

TURNER, J. S. 1974 Double-diffusive phenomena. *Ann. Rev. Fluid Mech.* **6**, 37.

VILLANOVE, R., GUYON, E., MITESCU, C. & PIERANSKI, P. 1974 Mesure de la conductivité thermique et détermination de l'orientation des molécules à l'interface nématique isotrope de MBBA. *J. Phys.* **35**, 153.

WEISFREID, G., POMEAU, Y., DUBOIS, M., NORMAND, C. & BERGÉ, P. 1978 Critical effects in Rayleigh–Bénard convection. *J. Phys.* **39**, 725.